Composites: Part A 51 (2013) 99–107

Contents lists available at SciVerse ScienceDirect

Composites: Part A

journal homepage: www.elsevier.com/locate/compositesa

Defects in woven preforms: Formation mechanisms and the effects of laminate design and layup protocol ☆

James S. Lightfoot *, Michael R. Wisnom, Kevin Potter

University of Bristol, Advanced Composites Centre for Innovation and Science, Queen's Building, Bristol BS8 1TR, United Kingdom

ARTICLE INFO

Article history:
Received 17 February 2013
Received in revised form 4 April 2013
Accepted 5 April 2013
Available online 19 April 2013

Keywords:
A. Preform
B. Defects
D. Non-destructive testing
E. Layup

ABSTRACT

Defects, such as in-plane waviness and out-of-plane tow wrinkles, cause significant reductions in the mechanical performance of RTM-manufactured composite parts based on woven preforms. To avoid this problem and achieve a greater acceptance rate in industrial processes, the mechanisms behind these defects must be understood. This paper presents a mechanism for the formation of these defects, which is supported through layup trials of woven preforms. Laminate design and layup protocol were found to be significant drivers behind the mechanism. Defect severity can be controlled through intelligent stacking sequence design and reducing ply bridging by manual forming actions and ply–ply adhesion during layup.

© 2013 The Authors. Published by Elsevier Ltd. All rights reserved.

1. Introduction

A number of industries, including aerospace and automotive, manufacture composite parts through processes based on resin transfer moulding (RTM), which relies on woven and/or tightly bound reinforcements being manually laid up into a forming mould. This preform is then infused with resin and subsequently cured in the RTM mould, thus forming the composite part. In order for parts to meet the acceptance criteria they must be largely defect-free, particularly from defects such as in-plane waviness and out-of-plane wrinkling of plies, which are likely to reduce the mechanical properties of the final part [1–3]. To reduce failure rates of composite parts an understanding of the mechanisms behind the formation of such defects is essential. Drivers such as laminate design and process parameters behind such mechanisms must also be characterised.

Defects observed in composite parts should be categorised into two groups; design induced defects and process induced defects [4]. The former being defects formed due to complex tool geometry or choice of fabric, such as out-of-plane curvature leading to wrinkles on external corners. Avoidance of such defects requires redesign of the part, tooling or materials and is therefore expensive for an industrial practice. Understanding of the core mechanisms behind process induced defects is of interest, since small changes in part manufacture, such as layup technique, can be achieved on an existing manufacturing line.

Currently known mechanisms behind defect formation in woven cloths pay particular attention to the ability of the cloth to map to the surface of a tool with complex geometry. Early work was carried out by Tam and Gutowski [5], in which the onset of tow wrinkling was found to coincide with the angle between warp and weft tows reaching a critical limit. Further experimental work examined the relationship between the shear angle and the onset of tow wrinkling [6], which established a number of fabric parameters behind this mechanism. Such parameters included friction, tow size and spacing.

The angle at which wrinkling occurs, the locking angle, has been experimentally derived by a number of researchers using a picture frame test. This in-plane shear behaviour is well characterised and has received much attention in both dry and prepregged cloths, such as, but not limited to, References [7–10]. the use of blank holders has been found to reduce the tendency of woven cloths to form wrinkles during manufacturing [11]. More recently, efforts have been made to model this process to examine the effect of constituent properties, finding the bending stiffness of the tows plays the main role in the shape of a wrinkle [12].

A mechanism for the formation of through-thickness ply wrinkles in unidirectional prepreg was proposed by Lightfoot et al. [13], which was based on the frictional shear between plies during consolidation. During the process of layup, stiff plies tend to bridge tooling radii, which then drag compliant plies into the radii as the laminate consolidates when a slip layer is used between tool and the prepreg layers. The result of this mechanism is ply wrinkling and severe in-plane fibre waviness.

The aim of this paper is to examine the mechanism presented in Ref. [13] in the context of dry woven cloths, which has not

☆ This is an open-access article distributed under the terms of the Creative Commons Attribution License, which permits unrestricted use, distribution, and reproduction in any medium, provided the original author and source are credited.

* Corresponding author. Tel.: +44 1173315504.
E-mail address: J.S.Lightfoot@bristol.ac.uk (J.S. Lightfoot).

1359-835X/$ - see front matter © 2013 The Authors. Published by Elsevier Ltd. All rights reserved.
http://dx.doi.org/10.1016/j.compositesa.2013.04.004

previously been addressed. It also aims to establish the mechanisms behind two of the most common defects observed in woven cloth preforms and to examine the effects of laminate design and layup protocol on such defects in unidirectional (UD) and biaxial satin cloths. The two defects in question are in-plane tow waviness and deformation of 90° tows that lead to ply wrinkles.

2. The mechanism

The core mechanism of bridged plies from Ref. [13] is expected to apply, regardless of reinforcement type. Fig. 1 shows a free body diagram of a two ply example, in which a compliant ply, such as a 90° ply, is laid onto the tool followed by a stiffer ply, such as a 0° ply. The stiffer ply will tend to bridge over the radius, leading to differential shear forces along the length of each ply. Movement of the stiff ply into the radius during consolidation causes a frictional shear force where the two plies meet. If this frictional shear force is greater than the frictional shear force between the tool and the first ply [14], movement of the first ply relative to the tool surface can occur. Consolidation of the plies into the corner results in the first ply being in a local state of compression at the radius, which results in defects being formed.

The mechanisms leading to the formation of two defects, in-plane tow waviness and tow crushing, are discussed in turn.

2.1. In-plane tow waviness

Tows oriented at 0°, either in UD or biaxially woven cloths, can form in-plane tow waviness. This is a result of the compression in the tow due to consolidation, combined with the constraint imposed by the next ply; movement in the out-of-plane direction is not permitted. Without this ply, through-thickness displacement is more likely to occur. Fig. 2 shows the mechanism of in-plane waviness formation. Compression of a tow will cause buckling in the *z*-direction due to the width of the tow being greater than its thickness. However, if displacement in this direction is constrained by the plies above it consolidating, the tow cannot buckle into the *z*-direction. Instead displacement in-plane occurs, which results in in-plane tow waviness.

2.2. Ply wrinkles

UD plies comprised of primarily 90° tows will also be subject to compressive loads. Fig. 3 shows the mechanism for tow deformation, in which the compressive load leads to rotation of the 90° tows around their centroidal axes to account for the excess length of the ply in the radius. An intermediate state is shown in Fig. 3, in which the excess length has been accounted for, however consolidation has not occurred. Consolidation of the ply stack against the tool surface causes deformation of the rotated 90° tows. Unaffected tows will remain elliptical whilst the deformed tows will not. This process results in the in-plane waviness of the 0° binder tows, and reduces the overall width of the rotated 90° tows. Plies that contain deformed 90° tows will be henceforth referred to as "ply wrinkles," please note that the orientation of these tows has not been affected; all remain at 90°.

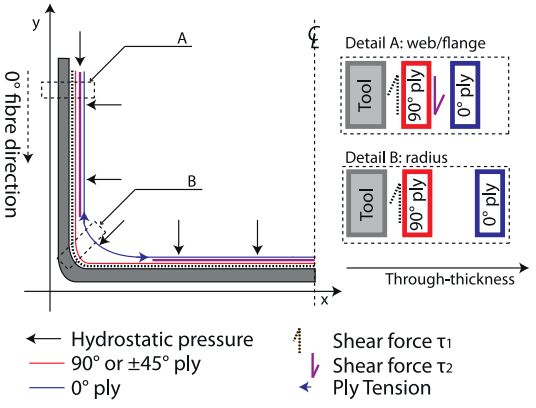

Fig. 1. Free body diagram showing the result of a bridged ply over a well-formed ply in one half of a U-shaped tool [13]. (For interpretation of the references to colour in this figure legend, the reader is referred to the web version of this article.)

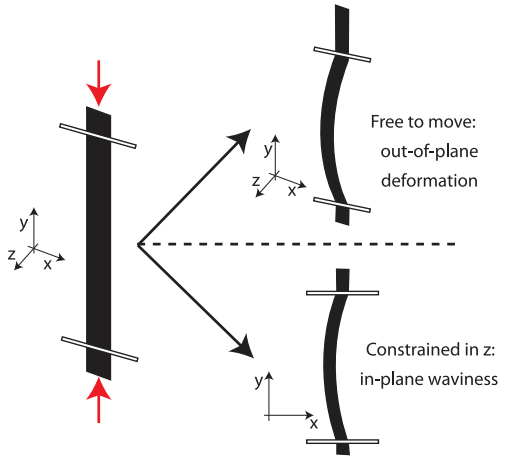

Fig. 2. In-plane tow waviness forms in cloths with 0° tows running along radii due to excess length and the constraint imposed by neighbouring plies. Compression (shown by arrows) is the result of a consolidation of bridged plies into a tooling radius. A single tow is shown, in which a compressive load leads to buckling, depending on the presence of a *z* direction constraint. (For interpretation of the references to colour in this figure legend, the reader is referred to the web version of this article.)

2.3. Misalignment of biaxial woven cloth

The deformation of biaxial cloth depends on the orientation at which the ply has been cut. Plies with warp and weft tows at ±45° deform through shearing. In compression the shearing process increases the angle between warp and weft tows through increasing the overall width of the ply if the cloth is unconstrained. Plies containing tows at 0/90° will abide by the mechanism discussed in Section 2.1, forming in-plane waviness in the 0° tows. This will in turn cause lateral movement of the 90° tows.

3. Materials and method

In order to corroborate the mechanisms suggested, preforms were manufactured using woven material laid up into a U-shaped aluminium tool. Geometry of the tool is shown in Fig. 4. The distance between the radii of this tool may increase the tendency for defects to arise under compaction pressure. The use of a tool with a longer "web" may have reduced this effect.

The materials used included a low crimp "uniweave" and a satin cloth, which has a woven tracer fibre. The uniweave is a highly unbalanced cloth, comprising of unidirectional carbon fibre tows, providing the stiffness and strength to the preform, and glass fibre binder weft yarns. The warp carbon tows comprise roughly 98% of the preform. This cloth type will be referred to as "UD" henceforth. Deformation of the satin cloth prior to layup was minimised by cutting on a vacuum-assisted computer-controlled ply cutter. The prismatic nature of the tool resulted in no shear of the cloth during placement.

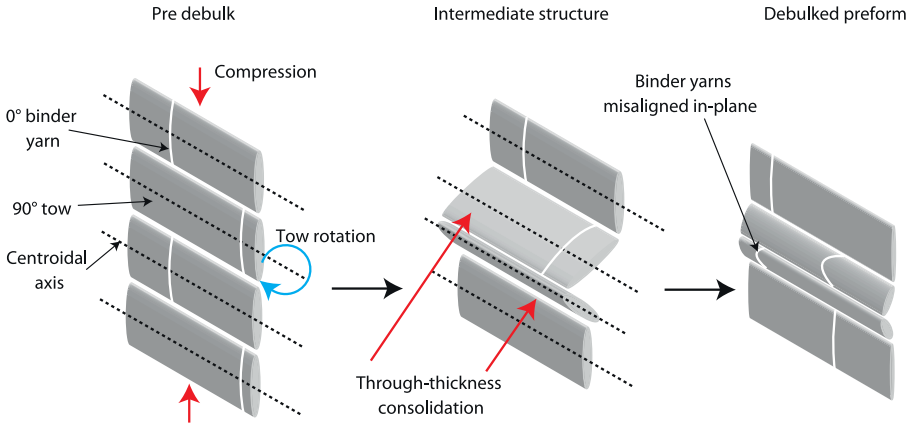

Fig. 3. Tow wrinkling of 90° tows and in-plane waviness of 0° binder yarns is a result of compressive forces and subsequent tow rotation. Consolidation causes further deformation of the tows. (For interpretation of the references to colour in this figure legend, the reader is referred to the web version of this article.)

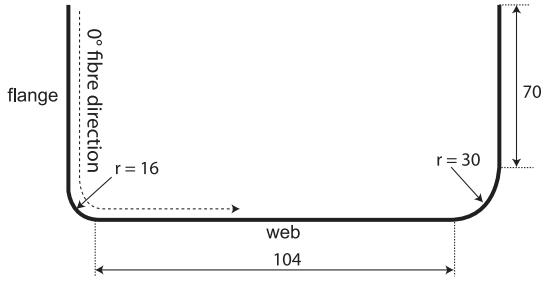

Fig. 4. Geometry of U-shaped aluminium spar tool used in this paper. 0° Fibre direction has been defined.

Plies were individually laid into the female mould, ensuring the second and subsequence plies were positioned well to the first. The ply edges were used as references for the positioning process. A vacuum bag was then constructed over the cloth stacks. The vacuum bag did not include pleats. Release film was not used between tool surface and the first ply of the stack, although Frekote release agent had been applied to the aluminium tool surface.

The UD cloth was surface treated with a thermoplastic powder binder, which was cured at an elevated temperature in a vacuum bag, resulting in a stiff, portable preform. Resulting "pre-laminates" were then mounted on a stand and photographed, with focus on the radii, where in most cases defects were formed. The UD cloth was cut at 0° and 90° orientations, whilst the satin cloth was cut into 0°/90° and ±45° plies.

The method of defect quantification used depended on the type and direction of the ply being examined. Due to each orientation having its own deformation mechanism, the morphology of the defects required their own metric.

Tows oriented at 0° typically formed waviness with the morphology of a half sinusoidal wave, and were assigned a waviness angle according to a function of the path length of the sine wave. Fig. 5 shows the rationale behind the metric, in which a half sinusoidal tow is simplified into a triangle. The angle of the tow is calculated according to Eq. (1), in which the "average angle" of the tow, θ, is a trigonometric function of the path length of the tow, ω, and the baseline length of the tow, β. Dimension β corresponded to the length between the aligned sections of each tow, highlighted in Fig. 5b. Whilst this is a simplification, it was found to be the most robust technique for calculating an angle for the tows due to some variation amongst the shapes observed. This method provided a convenient way of generalising the calculation, resulting in each data point being calculated in the same manner regardless of small differences in tow morphology.

$$\theta = \cos^{-1}\frac{\beta}{\omega} \tag{1}$$

The 0° tows in the satin cloths were quantified using Eq. (1). One photograph of each radius was taken, which was then cropped to an area 4000 × 800 pixels in size, which covered the area of the radius subject to defects. ImageJ was then used to measure the path lengths of each tow, which were passed through Eq. (1) to calculate the waviness angle.

In the case of 90° UD plies, both the misalignment angle of the 0° binder yarns and the relative width of the tows were taken as a metric (an undeformed tow has a relative width of 1). This was done because both of these were good indications of the severity of the wrinkle, which conventional 2D photography cannot show. The 0° binder yarns were measured using one of two techniques depending on the nature of the misalignment. Sinusoidally misaligned yarns were quantified using Eq. (1). In the case of yarns that were straight, but misaligned a simple "drag and measure" technique was carried out in ImageJ.

In the case of 90° UD cloth, the five tows covering each radius were interrogated for relative tow width and binder yarn misalignment. Whilst misaligned binder yarns are unlikely to affect material properties, they serve as a good indictor of tow compression due to excess length, and therefore a visual cue for a defect. Binder yarn misalignment and tow width were recorded at 15 sites along the 80 mm wide ply. Also recorded were the number of "crushed" tows, which is indicative of the severity of the ply wrinkle.

Two layup techniques were employed. Firstly, plies were laid into the tool and allowed to debulk naturally in a vacuum bag. No effort was used to adhere the plies to one another before the vacuum bag was constructed. This technique, referred to henceforth as "natural" layup resulted in the most severe bridging and was used as a worst case scenario.

Secondly, an industrial practice technique was adopted. This involved laying the first ply into the mould and fixing in place with a single spring-loaded clamp at the top of a flange. The second ply was then adhered to the first at the clamp position through use of a heat gun set at 400 °C, which melted the thermoplastic binder on the ply surface. The heat gun was used to adhere the ply along its length, which was done in conjunction with manual action of physically pushing the ply into the tooling radii. This was followed by a vacuum debulk for three hours at 125 °C. This technique, referred to as "forced" layup resulted in less bridging when compared to the natural method.

To cover aspects of laminate design, a number of ply orientation combinations were trialled. Initially, two ply pre-laminates were examined. Four ply pre-laminates were also investigated to

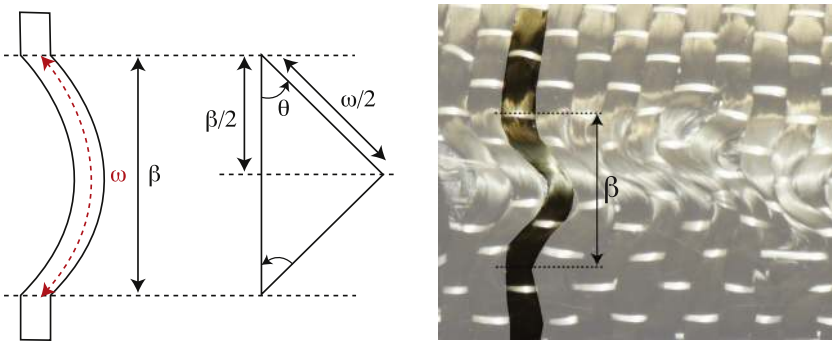

(a) Idealised tow morphology visualised as a triangle for trigonometric calculation.

(b) Actual tow morphology (single tow highlighted), with β dimension shown for reference.

Fig. 5. Metric applied to 0° tows was a function of the path length of the tow, ω, and the baseline length, β. (For interpretation of the references to colour in this figure legend, the reader is referred to the web version of this article.)

examine the effects of separating stiff plies with 90° plies. To compare datasets from different stacking sequences and layup techniques one-way analysis of variance (ANOVA) was performed, followed by passing the output from ANOVA through the *multcompare* algorithm in Matlab. This process shows whether the means from two or more populations are statistically different, at a 95% confidence level. Since ANOVA assumes equal variances an *F*-test was carried out first to examine the variances of the data.

X-ray computer tomography (CT) scanning was carried out at the National Composites Centre (NCC), Bristol, UK. A total of 1000 scans were carried out around the 360° rotation of the sample. A tungsten target was used to generate X-rays. An amorphous silicon detector was used, with dimensions 2000 × 2000 16 bit pixels. The scanning voltage used at the NCC was 100 kV (120 μA). A 250 ms exposure time was used. CT data was then reconstructed with Nikon CT Pro and visualised using VGMax Studio 2.1.

4. Defects observed in woven pre-laminates

4.1. Natural layup

Due to the severity of the radii in the tool relative to the size of the tows, defects were consistently manufactured using two and four ply pre-laminates. Fig. 6 shows the in-plane tow waviness observed in UD 0° and 0/90 satin plies (0° bias direction) at the tool surface. Tow misalignment was evident in satin cloths in which the 90° tows were the bias direction, as shown in Fig. 7a. The tracer fibre has been highlighted in this image, as well as the surrounding tows in red, green, blue and magenta. The highlighted tows show the sinusoidal waviness of the 0° tows in the sheared cloth. Ply wrinkling was observed in 90° UD plies, which has been shown in Fig. 7b. The presence of a wrinkle in 90° tows is indicated by the wrinkled tows having a smaller width than the unwrinkled tows, which is evident in Fig. 7b.

4.1.1. In-plane waviness

In-plane waviness was quantified for pre-laminates in which a 0° UD or 0/90 satin ply was laid into the mould first. Data between replicates for absolute mean misalignment in pre-laminates in which a 0° UD or a biaxial cloth with a 0° bias is at the tool surface for both radii was consistent. To show this consistency, Fig. 8 shows ANOVA data for both replicates of [0,0/90] pre-laminates debulked naturally, and represents typical replicate variability data. Passing this data through the *multicompare* algorithm in Matlab showed that for each tooling radius both data sets have means that are not significantly different.

Fig. 8 shows that each dataset is somewhat variable if one considers the total range of waviness angles. The source of the variability between each dataset is likely to be small, unconscious differences during hand layup. A previous study using prepreg showed that defect morphology can vary, despite the same stacking sequence and layup protocol being used [13].

Due to this consistency, matched replicate data was concatenated to calculate a single mean and standard error for each pre-laminate at each tool radius. Firstly, an *F*-test was carried out to check the variance of each matched replicate set was statistically the same, which was accepted at a 95% confidence level. ANOVA was then carried out to examine whether the means were statistically the same, which was also accepted. The process of concatenation was carried out to allow a more direction comparison of pre-laminate waviness angles.

Standard error provides an estimate of how variable the means will be if the experiment is repeated multiple times [15]. It provides the area over which the "true mean" of the data is likely to lie. This statistical method provides a good indication of the true

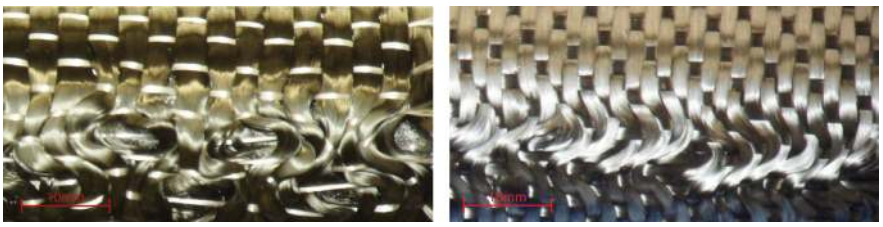

(a) 0° UD

(b) 0° bias 0/90 satin cloth

Fig. 6. In-plane tow waviness observed at a 16 mm radius in plies at the tool-part interface. (For interpretation of the references to colour in this figure legend, the reader is referred to the web version of this article.)

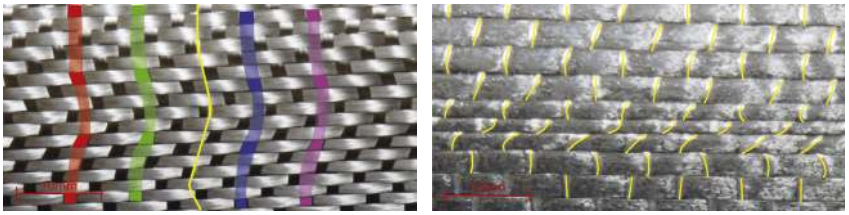

(a) Shearing, leading to tow misalignment in 90/0 satin cloth (90° bias). Tows highlighted (yellow-tracer).

(b) Ply wrinkle in 90°UD cloth, as well as 0° binder yarn misalignment. Binder yarns highlighted in yellow.

Fig. 7. Tow misalignment and ply wrinkling observed at a 16 mm radius in plies at the tool-part interface. (For interpretation of the references to colour in this figure legend, the reader is referred to the web version of this article.)

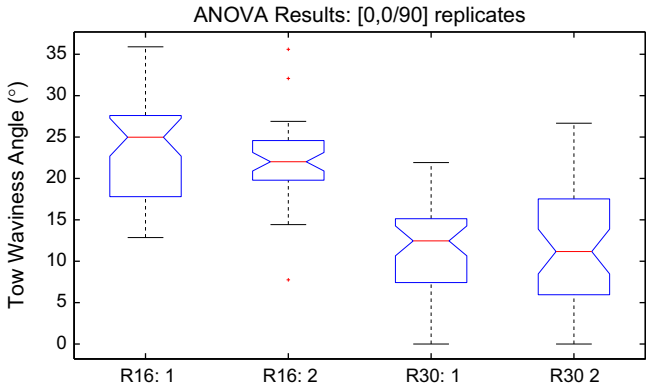

Fig. 8. ANOVA results for two replicates of [0,0/90] in boxplot form demonstrating consistency of data over replicates. X-axis labels refer to radius (mm) and replicate. Standard boxplot notation has been used (red line-median, blue horizontal lines-25th and 75th percentiles and whiskers-range). (For interpretation of the references to colour in this figure legend, the reader is referred to the web version of this article.)

mean, and therefore a method to compare the means of multiple samples. This standard statistical calculation is simply defined as the standard deviation divided by the square root of the number of measurements taken.

Fig. 9 summarises the data collected for pre-laminates in which a 0° UD or a biaxial cloth with a 0° bias is at the tool surface for both radii. The in-plane waviness is in most cases severe, with up to 24° calculated; in all cases the waviness observed at the 16 mm radius is more severe than at the 30 mm radius. The standard error bars show a good confidence in the calculated mean values. The [0,90] pre-laminate was defect free; all tows were at their intended alignments. Splitting up 0° plies with 90° plies, as shown in $[0,(90)_2,0]$, does not lead to a significant reduction in-plane waviness of the 0° tows; the mean waviness angle remains high at 20°.

4.1.2. Ply wrinkles

A CT image of a ply wrinkle in a 90° ply is shown in Fig. 10, in which Fig. 10a shows two tows that have formed a ply wrinkle. Fig. 10b shows a 2D slice of 10a, highlighting the deformation of the 90° tows.

Results for pre-laminates with 90° plies at the tool surface are summarised in Fig. 11. Examining the number of crushed 90° tows shows that two ply pre-laminates laid up using the natural technique are more susceptible to ply wrinkling at the 16 mm radius. The inclusion of two 0° plies in the $[90,(0)_2,90]$ pre-laminate, does not result in the defects becoming more severe; tows remain deformed at the 16 mm radius.

Also shown on Fig. 11 is data for the misalignment of the binder yarns and the relative width of the 90° tows. In all cases in Fig. 11,

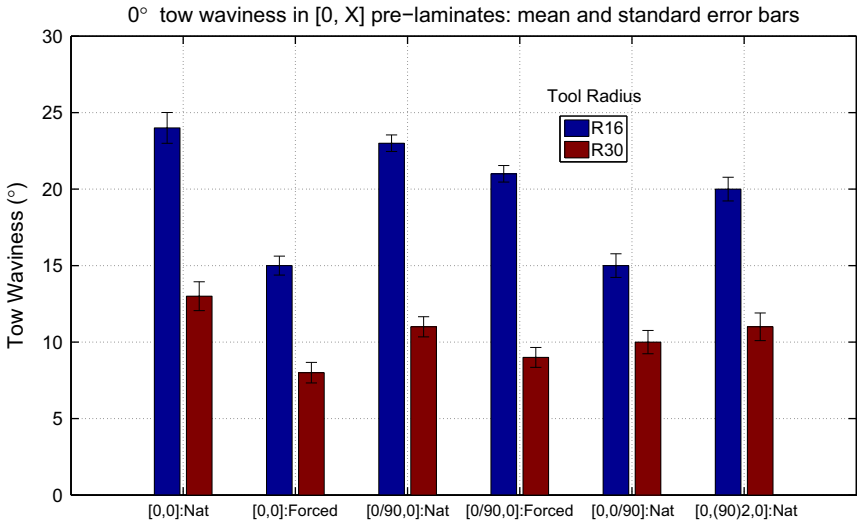

Fig. 9. Concatenated waviness data for pre-laminates in which 0° tows are at the tool surface; it is this ply that has been quantified in terms of in-plane waviness. Both natural and forced techniques are shown. Means and standard error bars are shown. Two replicates have been concatenated for each bar, representing $n = 60$ for UD 0° and $n = 100$ for biaxial cloth. [0,90] not shown due to aligned tows. (For interpretation of the references to colour in this figure legend, the reader is referred to the web version of this article.)

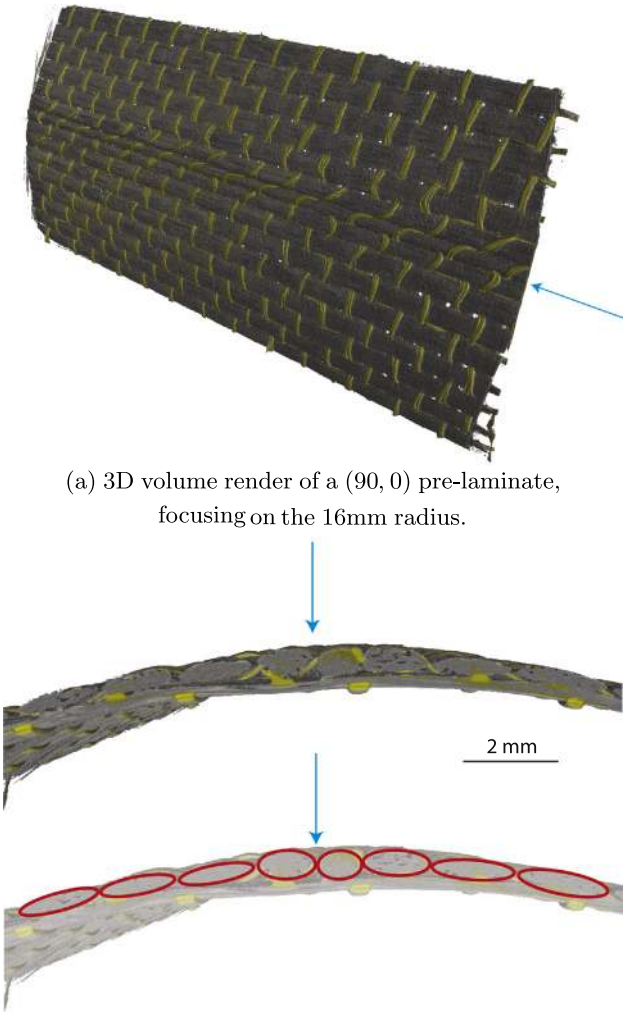

(a) 3D volume render of a (90, 0) pre-laminate, focusing on the 16mm radius.

(b) Top: 2D shot a ply wrinkle. Bottom: deformed morphology of tows highlighted using red ellipsoids.

Fig. 10. A CT scan for a 90° ply wrinkle. False colour imaging has been used to highlight 0° binder yarns in yellow. Blue arrow shows the location of the wrinkle in all panels. (For interpretation of the references to colour in this figure legend, the reader is referred to the web version of this article.)

the binder yarn misalignment is more severe at the 16 mm radius, regardless of the presence of a wrinkle. Examination of the 16 mm radius data shows that the presence of a ply wrinkle will increase the mean of the binder yarn misalignment.

Fig. 12 shows typical variability data for [90,0] and [90,$(0)_2$,90] pre-laminate datasets. The data for [90,0] shows a clear effect of tooling geometry on the relative width of the tow and binder yarn misalignment; the 16 mm radius is more severe. There also appears to be a loose inverse correlation between the relative width of the tow and the misalignment angle of the binder yarn.

4.1.3. Off-axis satin plies

In a similar process to 0° and 90° plies, the satin cloth was cut at ±45° orientations, followed by plies being laid up; ±45° plies were laid into the tool first, followed by UD plies. Regardless of the layup, defects were not observed for these pre-laminates; tows at the tool surface were neither misaligned nor deformed into ply wrinkles, unlike 0° and 90° UD cloth, respectively. Fig. 13 shows a typical ±45° surface ply at a 16 mm radius. Comparing this with Figs. 6 and 7 shows the significant differences in defect morphology between ±45° and other ply orientations. ImageJ was used to quantify the angle between warp and weft yarns, which were in all cases within ±4° of 90°.

From Section 4.1 the following trends can be recognised:

1. Plies with ±45° tows are not subject to either waviness or wrinkles (Fig. 13).
2. In two ply pre-laminates, 0° plies are likely to show significant tow waviness if the second ply deposited is stiff, such as another 0° ply or a 0/90 satin ply (Fig. 9).
3. 90° plies are likely to show ply wrinkling when combined with stiffer plies, as shown in Figs. 10 and 11 (layups [90,0] and [90,0/90]).
4. In two ply pre-laminates, tow waviness in 0° tows can be avoided by matching the ply with a compliant ply, such as a UD 90° ply (Fig. 9: layup [0,90]).
5. 90° plies cannot be used to "dilute" the effects of combining 0° plies. [0,$(90)_2$,0] in Fig. 9 shows a similar magnitude of in-plane waviness as [0,0], despite the 90° plies.
6. Satin cloths at a 0/90 orientation are subject to defects according to the same mechanism as the 0° UD cloths, the morphology of which depends on the bias direction of the cloth. Figs. 9 and 6b show in-plane waviness in the satin cloths to be severe and at a similar magnitude to 0° UD tows.

4.2. Manual drape and ply adherence

Fig. 14 shows an ANOVA boxplot output, focusing on the 16 mm tooling radius for two stacking sequences, [0,0] and [0/90,0], examining data for concatenated datasets from the forced and the matched data from the natural debulking method. Taking the data from the ANOVA test and running it through the *multcompare* algorithm in Matlab evaluates whether the means are significantly different from one dataset to another. This process showed that the forced layup technique reduced the severity of the waviness for the UD cloth. Despite the reduction, the magnitude of the in-plane waviness remains high. This process did not, however, statistically reduce the severity of waviness in the biaxial cloth.

[90,0] pre-laminates were also manufactured using the forced layup technique. A summary of the defects observed is given in Fig. 11, which shows that the industrial technique used has not resulted in ply wrinkles, whereas using the natural technique resulted in ply wrinkles consistently at the 16 mm tooling radius.

From layup trials using industrial techniques, the following trends have emerged:

1. The industrial technique hs not removed defects from pre-laminates, although the severity of the defects has been decreased in some cases.
2. 90° UD cloth does not suffer from severe ply wrinkles, shown in Fig. 11. Industrial practice has reduced the misalignment of binder yarns.
3. 0° UD cloth remains susceptible to in-plane tow waviness, although the severity has decreased, visible in Fig. 14.
4. 0/90 biaxial satin cloth is insensitive to layup procedure. The severity of in-plane waviness was unchanged by the forced layup technique (Fig. 14).

5. Discussion

The mechanism for the formation of ply wrinkles proposed by Lightfoot et al. focuses on prepreg-based laminates [13]. This study examines this mechanism using dry woven cloths, finding the mechanism to be in effect in this class of composite material. The morphology of the defects is significantly different, however. The mechanism relies on plies that tend to bridge over tooling radii during the layup process. During consolidation, these plies are

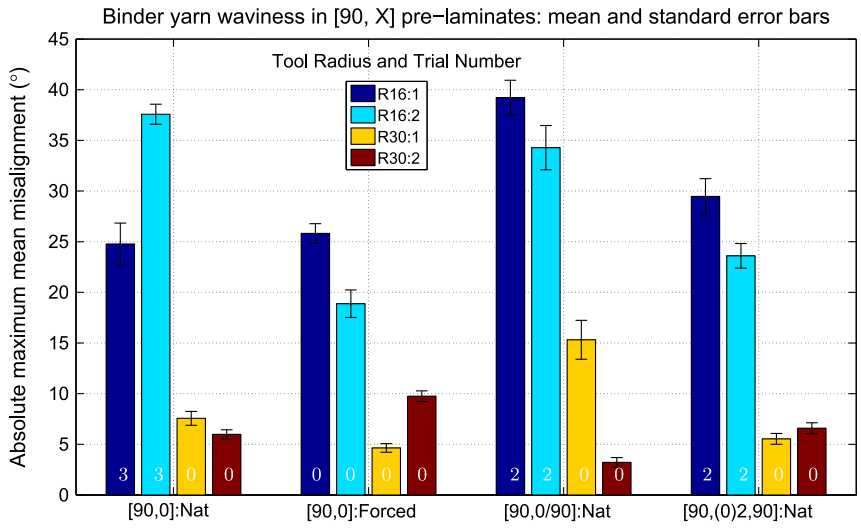

(a) 0° binder yarn misalignment: mean and standard error bars.

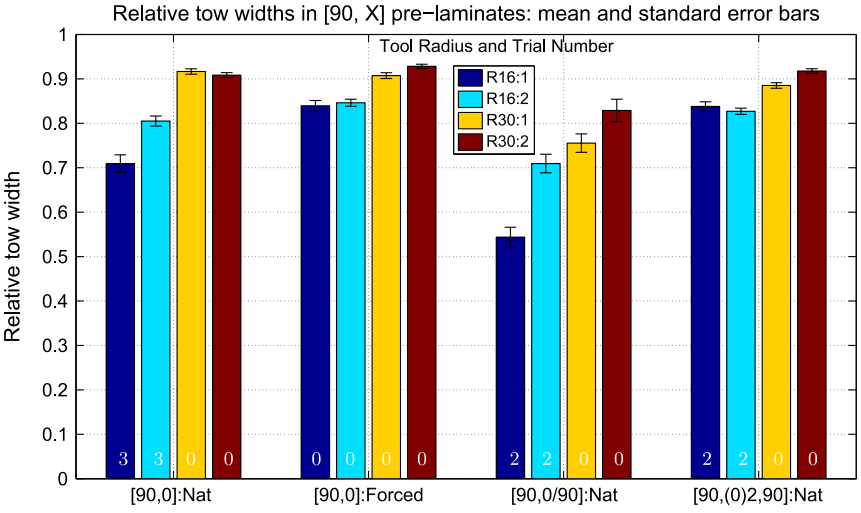

(b) 90° tow width: mean and standard error bars.

Fig. 11. Data for pre-laminates in which a 90° ply is at the tool surface. The tool-side ply was interrogated for both binder yarn misalignment and relative tow width of 90° tows. Shown in white is the number of 90° tows involved in a ply wrinkle at the defect site. $n = 75$ for each replicate. (For interpretation of the references to colour in this figure legend, the reader is referred to the web version of this article.)

forced into the radii of the tool. Due to the frictional shear force between the plies of cloth being greater than between the tool and first ply [14], the first ply is subject to compressive stresses in the region of the radius, according to Fig. 1.

The deformation mechanism of the tows depends on the type of reinforcement used as well as the orientation of the tows. The 0° UD and 0/90 woven tows will deform in-plane, forming waviness. 90° UD tows will rotate, deform and can form through-thickness ply wrinkles. The mechanism and deformation types have been supported through layup trials in a U-shaped tool. Implications of laminate design and process parameters have been explored through simple layup trials and quantification. The mechanism for the formation of in-plane tow waviness in Fig. 2 has been supported using photographic evidence in Fig. 6. The proposed mechanism for ply wrinkles and tow deformation in Fig. 3 has been supported using CT imaging in Fig. 10.

This research has also highlighted the possibility of using binder yarn misalignment as a visual indicator for tooling features that could lead to ply wrinkles in 90° plies. Misalignment of the binder yarns was observed in all cases of 90° plies at the tool surface, however the presence of severely misaligned yarns coincided with deformed tows in most cases. Simple visual inspection techniques can be powerful methods to quickly inspect parts for defects on an industrial manufacturing line.

Reference [13] showed a significant dependence of the mechanism on the presence of a slip layer between tool and prepreg; the presence of release film would consistently lead to wrinkles, whilst omission of this film would not lead to wrinkled laminates. This was due to the increased frictional shear between tool and prepreg than between prepreg and release film. Both techniques were employed in this body of research; defects were consistently produced in pre-laminates with and without a slip layer, showing a significant difference between prepreg and woven cloths in this regard. The key difference is likely to be the lack of "tack" when handling cloths when compared to uncured prepreg, which leads to a low friction coefficient with aluminium tooling.

The defects presented in this paper are likely to reduce the local compressive strength of the composite part. Experimental [16] and modelling based [1] efforts to calculate mechanical property reductions due to waviness have shown significant reductions in

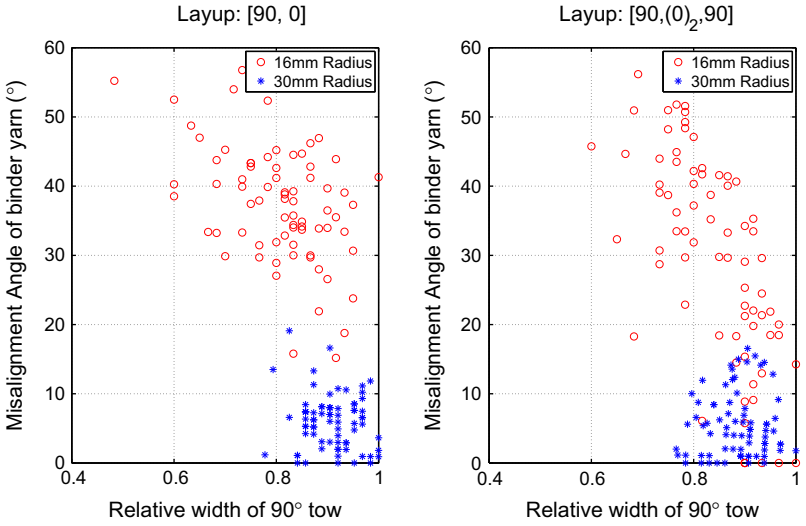

Fig. 12. Typical variability data for stacking sequences including 90° plies at the tool surface. (For interpretation of the references to colour in this figure legend, the reader is referred to the web version of this article.)

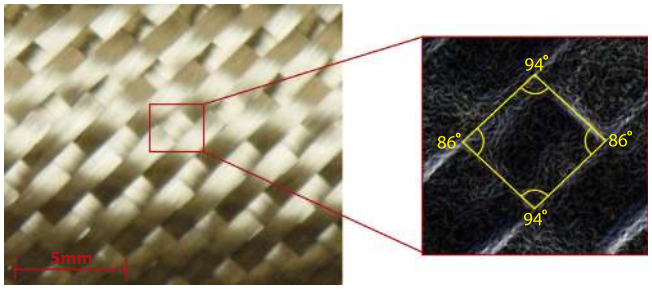

Fig. 13. Left: typical morphology of tows of ±45° satin cloth at a 16 mm radius. Right: zoomed in image of weft yarn. Edges have been highlighted. Angles have been quantified using ImageJ. (For interpretation of the references to colour in this figure legend, the reader is referred to the web version of this article.)

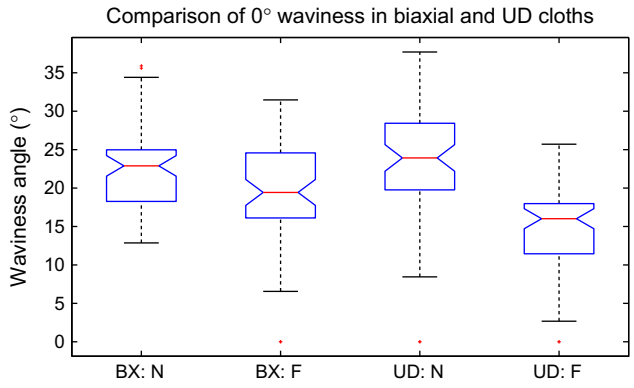

Fig. 14. Comparison of datasets for biaxial satin (BX) and UD cloths for in-plane waviness in the 16 mm radius. N: natural layup. F: forced layup. Standard boxplot notation has been used (red line-median, blue horizontal lines-25th and 75th percentiles and whiskers-range). (For interpretation of the references to colour in this figure legend, the reader is referred to the web version of this article.)

compressive strength as a result of fibre waviness. Many examples of experimental work in the literature focus on prepreg-based laminates in the context of fibre waviness and strength reductions; future work will be required to assess the implications of waviness on RTM-based components, furthering work such as Ref. [17].

5.1. Laminate design

Combining stiff plies at the tool surface with compliant plies, such as 90° UD, results in pre-laminates debulking without defects, shown by [0,90] in Fig. 9. This is because the compliant ply will not bridge the radius, regardless of how much the stiffer ply at the tool surface has bridged. This will form an intermediate structure in which a frictional shear stress will exist along the entire length of the two plies. Consolidation into the radius does not lead to defects in this case.

Combining 0° plies with other stiff plies, either 0° UD or 0/90 satin cloth, consistently forms in-plane tow waviness, highlighted by [0,0] and [0,0/90] in Fig. 9. Layups such as [90,0] in Fig. 11 show that the combination of 90° UD plies with stiffer 0° plies or 0/90 satin cloth forms wrinkles. A frictional shear stress will exist between the two plies where they are in contact. The length of each ply around the radius will not experience a ply–ply friction. Consolidation into the corner will place the ply at the tool surface into compression in the region of the radius. The excess length of the ply will be alleviated through in-plane deformation in the case of 0° tows, and tow rotation, deformation and wrinkles in the case of 90° UD tows.

Separation of 0° plies with 90° plies was trialled as a method to reduce waviness on the basis that [0,90] pre-laminates did not form in-plane waviness. The data for $[0,90_2,0]$ shown in Fig. 9 shows that the 90° plies could not "dilute" the shear interaction between the two 0° plies, and high levels of in-plane waviness were still observed. $[90,0_2,90]$ was trialled to examine whether multiple 0° plies would exacerbate defects when compared with [90,0] pre-laminates. Fig. 11 shows that this has not occurred.

The only case that did not result in defects, regardless of neighbouring ply orientation, was having a ±45° ply at the tool surface, which remained defect free despite being paired with a number of ply orientations and cloth types. It is likely that this observation is valid for prismatic moulds, in which shear deformation of ±45° plies is not required to map the ply to the tool surface. Non-prismatic moulds, such as industrial propeller blade formers, may result in defects in this cloth orientation. This result is also likely to be influenced by the width of the cloth; increasing the width of a UD prepreg ply cut at 45°, for example, increases the formation of wrinkles [18]. Further work should investigate the relationship between width of the cloth and the severity of defects observed.

The angle between warp and weft yarns in the ±45° cloth is a good indicator of the degree of compression subject to the ply. This compression is due to shear between plies generated during consolidation into the tooling radii. Angle quantification shown in Fig. 13 has shown that shear between warp and weft tows has occurred. Since these angles were typically 86–94° the shearing angles are not severe enough to reach locking angle of the cloth. Wrinkles observed in cited picture frame tests of similar materials [7–9] were not therefore observed.

This information has important ramifications when stacking sequences are designed for complex tooling geometries, particularly those with out-of-plane curvature and tight radii. Whilst the laminate will have to meet strength and stiffness requirements, designing the stacking sequence with the knowledge of complimentary ply combinations can reduce the tendency for defects to arise. Further work will be required to establish a set of layup guidelines using industrial former and preform geometry. Consolidation models simulating the onset of wrinkling and in-plane waviness would also be necessary. Such models could predict the onset of defect formation for a given tool surface geometry.

5.2. Process parameters: layup procedure

The procedure by which a preform is manufactured has a clear influence on the severity of defects formed. This investigation used an industrial technique of manually forming the plies, individually, into the radii of the tool whilst heating the plies with a heat gun. This process resulted in less bridging of plies over the radii firstly due to the plies being adhered to one another via a thermoplastic powder binder and secondly due to the manual process.

Ply wrinkles were not observed in [90,0] pre-laminates (Fig. 11). The mean misalignment of 0° binder yarns was also reduced, suggesting the amount of excess length being accommodated has reduced, which supports the mechanism suggested in this research. Fig. 14 has shown that the in-plane waviness in 0° UD plies is also reduced through this method. From the results presented it is evident that this process helps to control the formation of defects, but cannot eradicate them completely, which may be a consequence of the tooling geometry being relatively severe.

The type of reinforcement dictates the severity of defects. The defects in biaxial cloth were unaffected. The satin cloth is therefore more susceptible to defects than the UD cloth. Further work is required to discover the source of this difference and to examine a wider range of woven cloth types and weave structures. The study should also be expanded to examine alternative fabrics, such as loosely knitted cloths, since different types of fabric may give different results.

This exercise has shown that layup procedure is an important factor to consider during preform manufacture prior to resin infusion. Decreasing the bridging over tool radii through deliberate and careful manual forming and preform adherence are powerful techniques that are able to reduce defect rates in preforms.

6. Conclusions

From the work presented in this paper a number of conclusions can be drawn. Both laminate design and simple layup technique changes can have implications on the formation of defects in RTM preforms, such as in-plane waviness and ply wrinkles. The combination of plies, such as 0° UD plies with other 0° UD plies, consistently leads to defects due to the plies bridging the radii of the tool. This is due to the tool-side ply being placed in a state of compression during consolidation of the plies into tooling radii. Combining 0° plies with compliant 90° plies does not result in defects. Laying up ±45° plies at the tool surface also results in defect-free pre-laminates. The layup procedure also has a significant effect on the nature and severity of defects formed. Reducing the severity of ply bridging at tool radii through manual forming actions and ply–ply adherence is a simple technique that has removed through-thickness wrinkles in 90° UD cloth, as well as reducing the severity of in-plane waviness in 0° UD cloth. Whilst this process reduces the severity of defects, it cannot eradicate them completely.

Acknowledgments

The work presented in this paper is financially supported by EPSRC Grant No. EP/G036772/1 (as part of the Advanced Composites Centre of Innovation and Science Doctoral Training Centre) and Dowty Propellers, Part of GE Aviation. The author would also like to acknowledge Yusuf Mahadik for assistance with the CT scanning.

References

[1] Hsiao HM, Daniel IM. Effect of fiber waviness on stiffness and strength reduction of unidirectional composites under compressive loading. Compos Sci Technol 1996;56:581–93.
[2] Hayman B, Berggreen C, Pettersson R. The effect of face sheet wrinkle defects on the strength of FRP sandwich structures. J Sandwich Struct Mater 2007;9(4):377–404.
[3] Bloom LD, Wang J, Potter KD. Damage progression and defect sensitivity: an experimental study of representative wrinkles in tension. Compos Part B – Eng 2013;45(1):449–58.
[4] Potter K, Khan B, Wisnom M, Bell T, Stevens J. Variability, fibre waviness and misalignment in the determination of the properties of composite materials and structures. Compos Part A – Appl Sci Manuf 2008;39(9):1343–54.
[5] Tam A, Gutowski T. The kinematics for forming ideal aligned fibre composites into complex shapes. Compos Manuf 1990;1(4):219–28.
[6] Prodromou A, Chen J. On the relationship between shear angle and wrinkling of textile composite preforms. Compos Part A – Appl Sci Manuf 1997;28A:491–503.
[7] Rozant O, Bourban P, Manson J. Drapability of dry textile fabrics for stampable thermoplastic preforms. Compos Part A – Appl Sci Manuf 2000;31(11):1167–77.
[8] Potter K. Bias extension measurements on cross-plied unidirectional prepreg. Compos Part A – Appl Sci Manuf 2002;33(1):63–73.
[9] Sharma SB, Sutcliffe M, Chang SH. Characterisation of material properties for draping of dry woven composite material. Compos Part A: Appl Manuf 2003;34:1167–75.
[10] Harrison P, Abdiwi F, Guo Z, Potluri P, Yu WR. Characterising the shear–tension coupling and wrinkling behaviour of woven engineering fabrics. Compos Part A – Appl Sci Manuf 2012;43:903–14.
[11] Lee JS, Hong SJ, Yu WR, Kang TJ. The effect of blank holder force on the stamp forming behavior of non-crimp fabric with a chain stitch. Compos Sci Technol 2007;67:357–66.
[12] Boisse P, Hamila N, Vidal-Salle E, Dumont F. Simulation of wrinkling during textile composite reinforcement forming. Influence of tensile, in-plane shear and bending stiffnesses. Compos Sci Technol 2011;71:683–92.
[13] Lightfoot JS, Wisnom MR, Potter K. A new mechanism for the formation of ply wrinkles due to shear between plies. Compos Part A – Appl Sci Manuf 2013;49:139–47.
[14] Cornelissen B, Rietman B, Akkerman R. Frictional behaviour of high performance fibrous tows: friction experiments. Compos Part A – Appl Sci Manuf 2013;44:95–104.
[15] Vaux DL. Know when your numbers are significant. Nature 2012;492(7428):180–1.
[16] Wisnom M, Atkinson J. Fibre waviness generation and measurement and its effect on compressive strength. J Reinf Plast Compos 2000;19(2):96.
[17] Holmberg JA, Berglund LA. Manufacturing and performance of RTM U-beams. Compos Part A – Appl Sci Manuf 1997;28A:513–21.
[18] Potter K. In-plane and out-of-plane deformation properties of unidirectional preimpregnated reinforcement. Compos Part A – Appl Sci Manuf 2002;33:1469–1477.